J. Electrochem. Sci. Eng. **10(3)** (2020) 235-244; http://dx.doi.org/10.5599/jese.744

Open Access: ISSN 1847-9286
www.jESE-online.org

Original scientific paper

Electrochemical and quantum chemical parameters of (-)-(S)-9-fluoro-2,3-dihydro-3-methyl-10-(4-methyl-1-piperazinyl)-7-oxo-7H-pyrido[1,2,3-de]-1,4-benzoxazine-6-carboxylic acidas anti-corrosive agent for API 5L X-52 steel

Fidelis E. Abeng[1,2,✉], Magdalene E. Ikpi[2], Victor E. Okpashi[3], Onumashi A. Ushie[4] and Mbang E. Obeten[1]

[1]*Material and Electrochemistry Research Group, Department of Chemistry, Cross River University of Technology, Calabar, P. M. B 1123 Calabar, Nigeria*
[2]*Corrosion and Electrochemistry Research Laboratory, Department of Pure and Applied Chemistry, University of Calabar, P.M.B. 1115 Calabar, Nigeria*
[3]*Department of Biochemistry, Cross River University of Technology, P. M. B.1123 Calabar, Nigeria*
[4]*Department of Chemical Science, Federal University Wukari, Nigeria*

Corresponding author: ✉fidelisabeng@yahoo.com

Received: November 1, 2019; Revised: January 5, 2020; Accepted: January 6, 2020

Abstract

The inhibitive action of (-)-(S)-9-fluoro-2,3-dihydro-3-methyl-10-(4-methyl-1-piperazinyl)-7--oxo-7H-pyrido[1,2,3-de]-1,4-benzoxazine-6-carboxylic acid (Levaquin) on API 5L X-52 steel in 2 M HCl solution was investigated using potentiodynamic polarization method and quantum chemical study. Levaquin drug showed good inhibition efficiency of 88 and 95 % at 303 and 323 K, respectively. The results of experimental measurements revealed that Levaquin drug works as a mixed type inhibitor. Langmuir thermodynamic model was tested to describe the mode of inhibitor adsorption on the steel surface. The quantum chemical calculations confirmed the efficacy of Levaquin drug as a corrosion inhibitor.

Keywords

Corrosion; density functional theory; potentiodynamic polarization; organic inhibitor; adsorption.

Introduction

Corrosion is a destructive attack on a material caused by its reaction with environment. The severe consequence of corrosion has become a problem to the society. Corrosion causes waste of valuable resources, loss or contamination of products, and reduction in efficiency of the cost maintenance. Corrosion destroys the safety of metal structures and reduces technological progress.

Therefore, some control measures are needed to be implemented in order to inhibit corrosion, thereby prolonging the life span of metal structures. Use of organic corrosion inhibitors is the most efficient and economical approach among all anticorrosive methods. These inhibitors, however, cannot be used for large scale corrosion inhibition because of the growing ecological awareness about their high hazardous environmental implication [1]. Thus, some non- or low-toxic alternatives must be developed to replace traditional hazardous inhibitors. In recent years, some pharmaceutical drugs were recommended for such a purpose such as azithromycin [2], amoxicillin [3], cefixime [4], ciprofloxacin [5], amlodipine[6], oxytetracycline [7], doxycycline [8], norfloxacin [9], enrofloxacin [10], amifloxacin [11], pefloxacin [12], penicillin V [13], ampicillin [14], cloxacillin [15] and flucloxacillin [16]. All these pharmaceutical compounds are rich in heteroatoms like nitrogen, sulphur and oxygen, π bonds and/or aromatic rings, which are major adsorption centres in good corrosion inhibitors.

One of the most widely used metals is carbon steel, *i.e*. an alloy of iron and carbon which corrodes in the form of rusting. Rusting is the process of oxidation in which iron combines with water and oxygen to form corrosion products (rust). The present study aims to investigate (-)-(S)-9-fluoro-2,3-dihydro-3-methyl-10-(4-methyl-1-piperazinyl)-7-oxo-7H-pyrido[1,2,3-de]-1,4-benzoxazine-6-carboxylic acid (Levaquin) as corrosion inhibitor for API 5L X-5 carbon steel in 2 M HCl solution, using potentiodynamic polarization method and density functional theory (DFT) for the calculation of quantum chemical parameters.

Experimental

Acid-inhibitor solution preparation

Levaquin is an antibiotic drug used to treat several bacterial infections. It belongs to the class of fluoroquinolones and has molecular formula $C_{18}H_{20}FN_3O_4$ and molecular weight of 361.368 g/mol. The tablets of Levaquin were supplied from Peace land Pharmaceutical shop in Calabar-Nigeria. 500 mg of the drug was ground and dissolved in one liter of prepared 2 M HCl solution. The resultant solution was filtered to obtain the stock solution of concentration 500 ppm. Solutions of concentrations 50, 100, 200 and 300 ppm were prepared from this stock solution using serial dilution method [17,18].

Sample preparation

API 5L X-52 steel specimen with chemical composition shown in Table 1 was obtained from a cylindrical pipeline. The steel specimen was mechanically press cut into coupons of dimensions 1×1×1 cm. The coupons were polished using different grades of emery paper to obtain mirror polished surfaces. Copper wires were soldered to the coupons and mounted in epoxy resin to produce the working electrode. Prior to running electrochemical experiments, the coupons were once again polished, rinsed in distilled water, degreased in acetone and air dried.

Table 1. *Chemical composition of API 5L X-52 steel*

Element	C	Mn	P	S	Si	V	Cr	Ni	Mo	Al	Nb	Ti	Fe
Content, %wt	0.22	1.40	0.025	0.015	0.45	0.15	0.20	0.20	0.08	0.03	0.15	0.04	97.04

Electrochemical experiments

Potentiodynamic polarization experiments were carried out using a conventional three-electrode electrochemical cell assembly. Steel coupons with an exposed surface area of 1 cm^2 was used as the working electrode, saturated calomel electrode (SCE) as the reference electrode and platinum plate

as the counter electrode. The polarization measurements at 303 and 323 K, as well as estimations of corresponding polarization resistance values were performed using Gamry electrochemical analyzer. Potentiodynamic current-potential curves were recorded by changing the electrode potential automatically at the scan rate of 0.5 mV s^{-1}, from 0.25 V below to 0.60 V above the corrosion potential (E_{corr}). Before each run, the working electrode was immersed in the test solution for 30 minutes to attain steady state. The corrosion rate (CR) of the metal was examined through the corrosion current density (j_{corr}) using the equation

$$CR = \frac{K j_{corr} EW}{d} \quad (1a)$$

where K is conversion factor (3272 mm A^{-1} cm^{-1} y^{-1}), EW is equivalent weight of corroding metal in g equivalent, and d is density of the metal in g cm^{-3}. The inhibition efficiency (IE) was evaluated from j_{corr} values using the following equation [19-21]

$$IE = \frac{j_{corr(blank)} - j_{corr(inh)}}{j_{corr(blank)}} 100 \quad (1b)$$

where $j_{corr(blank)}$ and $j_{corr(inh)}$ are corrosion current densities measured in the blank solution and solution containing inhibitor, respectively.

Quantum chemical study

The density functional theory (DFT) was used for the quantum chemical calculations. Materials Studio 4.0 software with a basis set of 6.311 G and hybrid functional of B3LYP were used to treat the exchange-correlation interaction of electrons.

Results and discussion

Potentiodynamic polarization measurements

Polarization plots forAPI 5L X-52 steel coupons measured in 2 M HCl solution in the absence and presence of different concentrations of Levaquin (50, 100, 200, 300 and 500 ppm) and at two temperatures (303 and 323 K) are presented in Figures 1 and 2.

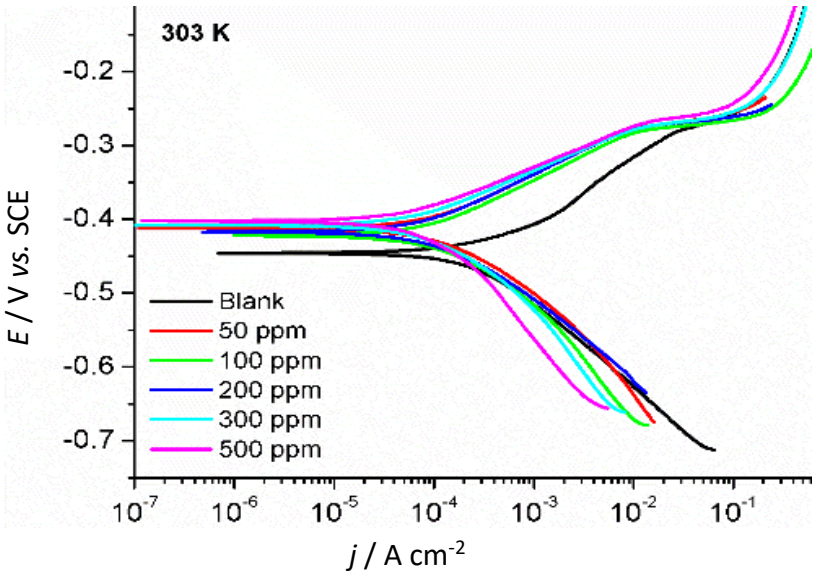

Figure 1. *Potentiodynamic polarization curves for carbon steel in 2 M HCl in the absence and presence of denoted concentrations of Levaquin at 303 K*

In both cases, cathodic and anodic branches of Tafel polarization curves in the presence of Levaquin are shifted towards lower current density values, which may be a result of the adsorbed inhibitor molecules [10]. It can also be deduced from the plots in Figures 1 and 2 that the studied molecules inhibit corrosion by controlling both cathodic and anodic reactions, *i.e.* as mixed type inhibitor [19]. In other words, addition of inhibitor reduces anodic dissolution of API 5L X-52 steel and also retards the cathodic reaction. Electrochemical parameters deduced from the polarization curves measured at two temperatures are listed in Table 2.

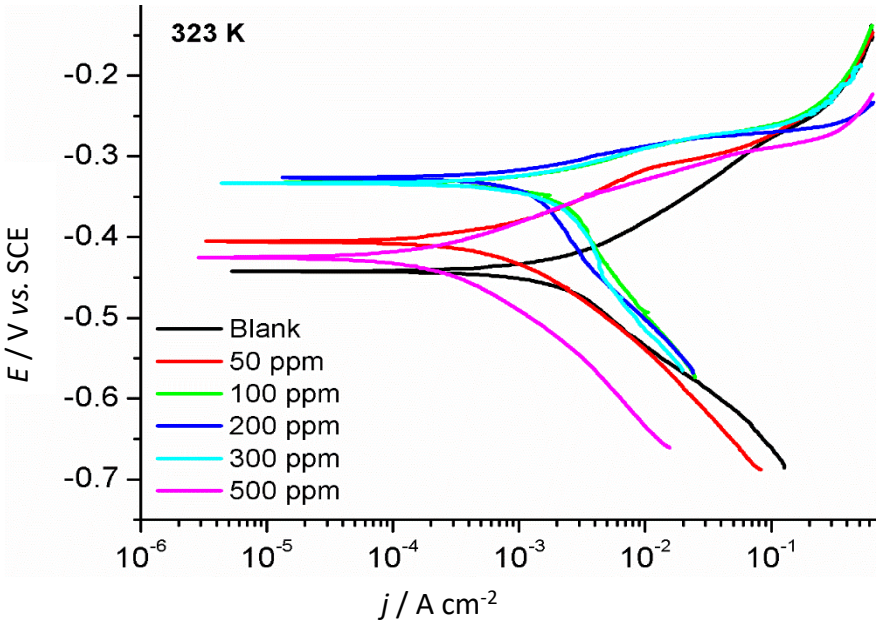

Figure 2. *Potentiodynamic polarization curves for carbon steel in 2 M HCl in the absence and presence of denoted concentrations of Levaquin at 323 K*

Table 2. *Electrochemical parameters obtained from Tafel plots*

T / K	*c* / ppm	β_a / mVdec^{-1}	β_c /mV dec^{-1}	E_{corr}/ mV	j_{corr} / µAcm^{-2}	CR, mm y^{-1}	R_p / Ω cm^2	θ	IE, %
303	Blank	102	454	-446	560	6.498	10633	--	--
	50	72	84	-412	98	1.137	22357	0.83	83
	100	71	84	-422	92	1.067	23137	0.84	84
	200	71	79	-417	80	0.928	24053	0.86	86
	300	64	90	-408	71	0.824	29029	0.87	87
	500	61	111	-402	65	0.754	41503	0.88	88
323	Blank	116	217	-442	3560	41.307	5433	--	--
	50	76	391	-333	3370	39.102.	9469	0.05	5
	100	61	249	-333	2040	23.670	5284	0.43	43
	200	53	541	-326	1770	20.537	22229	0.50	50
	300	74	100	-405	622	7.217	4752	0.83	83
	500	56	87	-425	188	2.181	8524	0.95	95

It can be observed from data in Table 2 that increase in the concentration of inhibitor results in decreased corrosion current density and corrosion rate, respectively. Simultaneous increase of inhibition efficiency (IE) or degree of surface coverage (θ), as well as polarization resistance (R_p) suggest that the studied compound blocked the available surface area of steel [19-23]. Note that the values of θ listed in Table 2 were determined using Equation (1b) divided by 100.

Effect of temperature

Temperature dependence gives some insight into the mechanism of inhibitor adsorption, because increase of inhibition efficiency of an inhibitor with increase in temperature predicts

chemical adsorption mechanism. At the other side, physical adsorption mechanism is feasible for decreasing inhibition efficiency at increasing temperature [3]. Hence lower inhibition efficiency at higher temperature (Table 2) suggests that a physical adsorption mechanism is generally operative in inhibition of steel corrosion by Levaquin, except at its highest concentration. Activation energy has also been used to predict the mechanism of adsorption as it depends on temperature. Generally, when the activation energy of an inhibitor is higher than that of the blank solution, physical adsorption mechanism is implied, whereas when the activation energy is lower than that of uninhibited solution, chemical adsorption is probable adsorption mechanism. Therefore, increase of the inhibition efficiency with increase in temperature corresponds to decrease of corrosion activation energy in the presence of inhibitor, suggesting thus the chemisorption mechanism. In reverse, decrease of inhibition efficiency with increase of temperature corresponds to increase in corrosion activation energy in the presence of inhibitor, suggests physical adsorption mechanism [23].

The apparent activation energies (E_a) for dissolution of API 5L X-52 steel in 2 M HCl in the absence and presence of the inhibitor were calculated from the condensed Arrhenius equation [24]:

$$\log\left(\frac{CR_2}{CR_1}\right)=\frac{E_a}{2.303R}\left(\frac{1}{T_1}-\frac{1}{T_2}\right) \quad (2)$$

where R is gas constant, while CR_1 and CR_2 are corrosion rates at temperatures T_1 and T_2, respectively. The calculated E_a values are listed in Table 3, showing generally higher values in presence of inhibitor than in blank solution, except for the highest concentration of Levaquin. In agreement with previous observations on IE temperature changes, it seems that physisorption mechanism is operating at lower concentration of Levaquin. Heat of adsorption (Q_{ads}) was evaluated using the following equation:

$$Q_{ads}=2.303R\left[\log\left(\frac{\theta_2}{1-\theta_2}\right)-\log\left(\frac{\theta_1}{1-\theta_1}\right)\right]\left(\frac{T_1T_2}{T_2-T_1}\right) \quad (3)$$

where θ_1 and θ_2 are degree sof surface coverage at temperatures T_1 and T_2, respectively. The estimated values of Q_{ads} are also listed in Table 3. The negative values of Q_{ads} are consistent with an inhibitor that is physically adsorbed on the metal surface [23,25].

Table 3. *Calculated values of activation energy (E_a) and heat of adsorption (Q_{ads})*

c / ppm	E_a / kJ mol^{-1}	Q_{ads} / kJmol^{-1}	θ_1	θ_2
Blank	73.33	--	--	--
50	140.71	-57.71	0.83	0.05
100	122.57	-78.11	0.84	0.43
200	123.14	-72.53	0.86	0.50
300	86.42	-15.34	0.87	0.83
500	43.03	-35.07	0.88	0.95

Adsorption isotherm

A possible way of discussing the mechanism of corrosion inhibition is through consideration of adsorption of organic compounds. The adsorbed compounds block the surface of the metal from corrosive agents, reducing thus the corrosion process. Adsorption provides information about interaction among adsorbed molecules, as well as their interaction with the metal surface. Adsorption isotherm is very important in proposing the mechanism of heterogeneous organo-electrochemical reaction on solid surfaces [26]. Different adsorption isotherm models were fitted

to the experimental data, and it was found that Langmuir adsorption isotherm fitted well to the experimental data (Figure 3). Langmuir adsorption isotherm is defined as

$$\frac{c}{\theta_2} = \frac{1}{K_{ads}} + c \quad (4)$$

where c is bulk concentration of adsorbed (inhibitor) species, while K_{ads} is equilibrium adsorption constant (L mol^{-1}), equal to the reciprocal of the intercept of straight line in Figure 3.

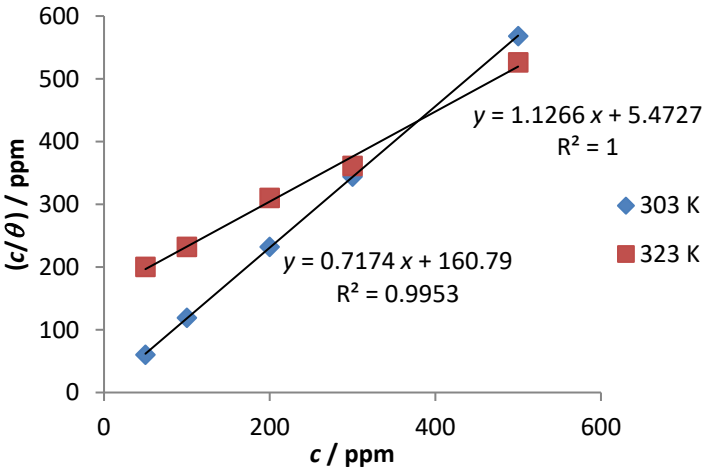

Figure 3. *Langmuir adsorption isotherm plot for the adsorption of Levaquin on API 5L X-52steel in 2 M HCl*

As shown in Table 4, the values of slopes and correlation coefficient (R^2) illustrate that at both temperatures, the experimental data agree very well with linear relationships. The thermodynamic adsorption parameter known as free energy of adsorption (ΔG_{ads}) was calculated at different temperatures using the equation

$$\Delta G_{ads} = -2.303RT \log 55.5\, K_{ads} \quad (5)$$

where 55.5 is concentration of water in mol L^{-1}, R is gas constant and T is absolute temperature

Table 4. *Calculated values of free energy of adsorption*

T / K	K_{ads}	Slope	ΔG_{ads} / kJ mol^{-1}	R^2
303	0.183	1.126	-18.41	0.995
323	0.0062	0.717	-66.87	1

The negative signs of ΔG_{ads} in Table 4 indicate that adsorption of Levaquin on the surface of API 5L X-52 steel is spontaneous. Generally, the values of ΔG_{ads} higher than -40 kJ mol^{-1} reflect chemisorption which involves charge sharing or transfer from inhibitor molecules to the metal surface to form a coordinate bond type, while values of ΔG_{ads} below -40 kJ mol^{-1} suggest electrostatic interaction between metal surface and charged organic molecules in the bulk of the solution identified as physisorption [23]. The calculated ΔG_{ads} values presented in Table 4 are between -18.41 and -66.87 kJ mol^{-1}, indicating that the adsorption mechanism of Levaquin on API 5L X-52 steel in 2 M HCl solution is physical adsorption at 303 K and chemical adsorption at 323 K.

Quantum chemical calculations

Quantum chemical calculations were employed to gain insight into the inhibition mechanism of Levaquin drug by examining the structure-reactivity correlation of the compound [1,19]. Figure 4 shows a complete geometric optimization of the studied molecule, while Figure 5 displays the frontier molecular orbitals namely, the highest occupied molecular orbital (HOMO) and the lowest

unoccupied molecular orbital (LUMO), present in studied compound. The calculated quantum chemical parameters obtained according to [16-24] are listed in Table 5.

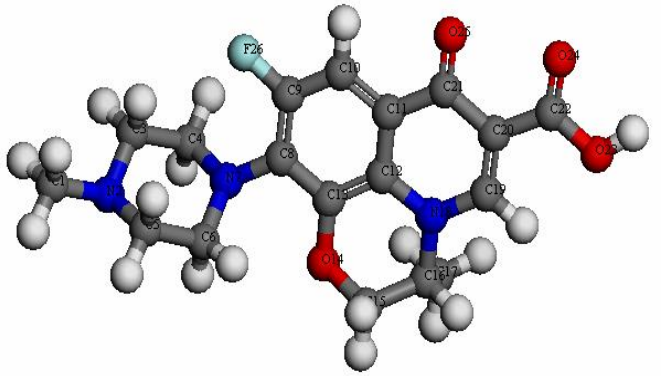

Figure 4. *Optimized structure of Levaquin molecule*

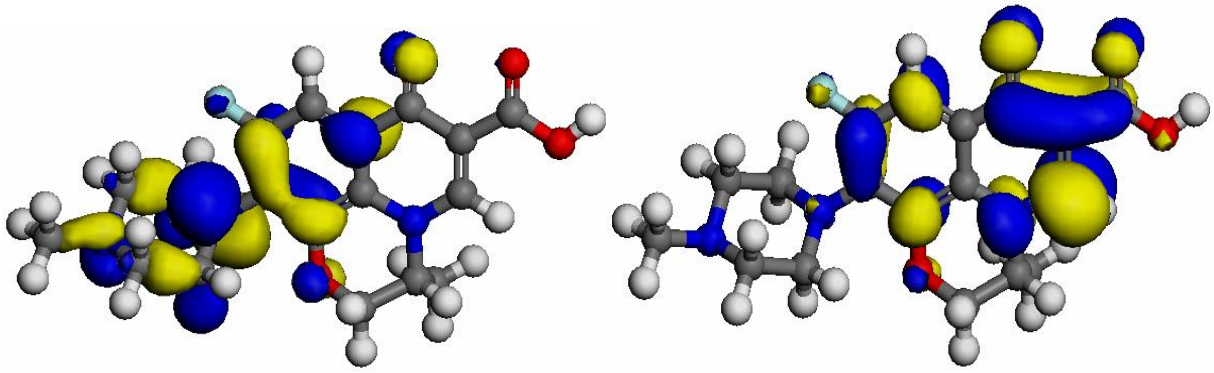

HOMO LUMO

Figure 5. *Frontier molecular orbital (HOMO and LUMO) structures of Levaquin*

Table 5. *Calculated quantum chemical parameters for Levaquin*

E_{HOMO} /eV	E_{LUMO} /eV	ΔE / eV	IP, eV	EA, eV	χ /eV	η / eV	σ	μ / *D*	ω	ΔN /e
-6.817	-3.315	3.502	6.817	3.315	3.066	1.751	0.571	12.28	7.327	0.501

Frontier molecular orbital calculations

The values of energy of the highest occupied molecular orbital (E_{HOMO}) and energy of the lowest unoccupied molecular orbital (E_{LUMO}) were obtained from DFT analysis. E_{HOMO} is often connected with the electron donating ability of a molecule, while E_{LUMO} shows its electron accepting ability. According to the results presented in Table 5, higher energy value of E_{HOMO} reveals the ability of the studied molecule to donate electron to an empty molecular orbital. Thus, increase in E_{HOMO} value facilitates adsorption of inhibitor [26-27], while the energy of LUMO shows the potential of the molecule to accept electrons.

Energy gap

Energy gap can also be used to predict inhibition efficiency of a compound or to develop a theoretical model for explaining the structure and confirmation barrier in many molecular systems. Energy gap (ΔE) is calculated using the following equation [28-29];

$$\Delta E = E_{LUMO} - E_{HOMO} \quad (6)$$

From our study the value of ΔE in Table 5 is within the range of values of good corrosion inhibitors [29].

Ionization potential and electron affinity

Ionization potential (IP) is the maximum energy necessary to remove an electron from many electron atoms in a gas phase, whereas electron affinity (EA) is the energy released when an electron attaches to a gas phase atom. According to the following equations

$$IP = -E_{HOMO} \quad (7)$$

$$EA = -E_{LUMO} \quad (8)$$

IP is related to E_{HOMO} while EA is related to E_{LUMO}. The calculated values of IP and EA are listed in Table 5 [30-31].

Electronegativity

Electronegativity reflects the power of an electron or group of atoms to attract electrons towards itself. The Koopman's theorem was used to estimate the electronegativity (χ) of the studied compound using the following equation

$$\chi = ½(E_{HOMO} + E_{LUMO}) \quad (9)$$

The higher the value of χ, the more effective is the inhibitor and vice versa. Data in Table 5 shows that χ value is within the range of effective inhibitors. These results agree with the experimental results of other studies [24,31].

Global hardness and softness

Global hardness (η) measures the resistance of an atom to charge transfer, whereas global softness (σ) describes the capacity of an atom or group of atoms to receive electrons [3,25]. The expressions for η and σ are given as follows

$$\eta = ½(E_{HOMO} - E_{LUMO}) \quad (10)$$

$$\sigma = 1/\eta \quad (11)$$

A hard molecule requires a large ΔE and a soft molecule requires a small ΔE. Soft molecules could therefore easily offer electrons to an acceptor system that make them more reactive than hard molecules. Furthermore, adsorption may occur at the point of a molecule where absolute softness is high [26,32]. Table 5 shows that the values of global hardness and global softness are within the range of effective corrosion inhibitors.

Dipole moment

The dipole moment (μ) is another index that is often used for the prediction of corrosion inhibition process. It is the measure of polarity in a bond, related to the distribution of electrons in a molecule. Therefore, inhibitors with high dipole moment form strong dipole-dipole interactions with the metal, ensuring a strong adsorption on the surface of the metal and leading to higher inhibition efficiency. It was observed that the dipole moment value for Levaquin shown in Table 5 correlates with the experimental results reported elsewhere [32-35].

Global electrophilicity index

Global electrophilicity index (ω) is estimated by combining the electrophilicity and chemical hardness parameters according to the following relation;

$$\omega = \frac{\chi^2}{2\eta} \quad (12)$$

A high value of electrophilicity index describes a good electrophile while a small value describes a good nucleophile [25-32]. The results presented in Table 5 show good correlations with the

experimental result of the study. The fraction of transferred electrons (ΔN) can be evaluated using the following equation:

$$\Delta N = \frac{W - \chi_{inh}}{2(\eta_{Fe} - \eta_{inh})} \quad (13)$$

where W is work function, χ_{inh} is electronegativity of inhibitor, while η_{Fe} and η_{inh} are the global hardness of Fe and inhibitor, respectively. The electronegativity χ was calculated using eq. (9), the value of η_{Fe} was taken as 0 eV mol^{-1}, while η_{inh} was calculated using eq. (10). To calculate ΔN, the work function with the value of W = 4.82 for Fe (110) surface was applied. For the value of $\Delta N > 0$, the electron transfer takes place between an inhibitor molecule and the metal surface, while for $\Delta N < 3.6$, the electron donating ability of an inhibitor molecule is increased. All the calculated values of this study are within the range of values already reported for some excellent corrosion inhibitors [27-28,36].

Conclusions

(-)-(S)-9-fluoro-2,3-dihydro-3-methyl-10-(4-methyl-1-piperazinyl)-7-oxo-7H-pyrido[1,2,3-de]-1,4-benzoxazine-6-carboxylic acid was tested as corrosion inhibitor process on API 5L X-52 steel in 2 M HCl solution, using potentiodynamic polarization and quantum chemical calculations. The following conclusions can be derived from the present study.

1. Inhibition efficiency of Levaquin increases with increase in its concentration.
2. Adsorption behaviour of Levaquin follows Langmuir adsorption isotherm and depending on temperature, reflects either physical or chemical adsorption mechanism. Levaquin is good corrosion inhibitor which acts as a mixed type inhibitor.
3. Results of calculations of quantum chemical parameters carried out in this study are in good agreement with experimental results.

References

[1] Y. Qiang, S. Zhang, B. Tan, S. Chen, *Corrosion Science* **133** (2018) 6-16.
[2] O. A. Abdullatef, *Journal of Advances in Chemistry* **11** (2015) 3642-3655.
[3] A. A. Siaka, N. O. Eddy, S. O. Idris, L. Magaji, Z. N. Garba, I. S. Shabanda, *International Journal of Modern Chemistry* **4** (2013) 1-10.
[4] I. Naqvi, A. R. Saleemi, S.Naveed, *International Journal of Electrochemical Science* **6** (2011) 146-161.
[5] I. A. Akpan, N. O. Offiong, *International Journal of Chemistry and Materials Research* **2** (2014) 23-29.
[6] I. A. Akpan, N. O. Offiong, *Chemical and Process Engineering Research* **26** (2014) 20-23.
[7] J. A. Von Fraunhofer, S. H. Stidhan, *Journal of Biomedical Engineering* **13** (1991) 424- 428.
[8] S. K. Shukla, M. A. Quraishi, *Corrosion Science* **52** (2010) 314-322.
[9] X. Pang, X. Ran, F. Kuang, J. Xie, B. Hou, *Chinese Journal of Chemical Engineering* **18** (2010) 337-345.
[10] S. Acharya, S. N. Upadhyay, *Transition Indian Institute of Metal* **57** (2004) 297-306.
[11] G. Gece, *Corrosion Science* **53** (2011) 3873-3898.
[12] A. S. Fouda, H. A. Mostafa, H. M. El-Abbasy, *Journal of Applied Electrochemistry*, **40** (2010) 163-173.
[13] N. O. Eddy, S. A. Odoemelam, *Advanced Natural and Applied Science* **2** (2008) 225-232.
[14] M. Abdallah, *Corrosion Science* **46** (2004) 1981-1996.
[15] A. S. Fouda, A. A. Al-Sarawy, F. S. Ahmed, H. M. El-Abbasy, *Corrosion Science* **51** (2009) 439-702.
[16] X. H. Pang, W. J. Guo, W. H. Li, J. D. Xie, B. R. Hou, *Science of China Series B Chemistry* **51** (2008) 928-936.
[17] P. O. Ameh, P. Ukoha, P. Ejikeme, N.O. Eddy, *Industrial Chemistry* **2** (2016) 2469-9764.
[18] S. Kumar, H. Vashisht, L. O.Olasunkanmi, I. Bahadur, H. Verma, G. Singh, I .B. Obot, E. E. Ebenso, *Scientific Reports* ***6*** (2016) 30937-30949
[19] J. Bhawsar, P.K. Jain, S. P. Jain, *Alexandria Engineering Journal* **54** (2015) 769-775.
[20] P. C. Okafor, E. E. Ebenso, U. J. Ekpe, *International Journal of Electrochemical Science* **5** (2010) 978-993.
[21] A. S. Fouda, G. E. Bekheit, M. W. El-Sherbari, *Journal of Bio and Tribo-Corrosion* **11** (2016) 1-16.
[22] N. O. Eddy, S. R. Stoyanov, E. E. Ebenso, *International Journal of Electrochemical Science* **5** (2010) 1127-1150.

[23] M. M. Kabanda, L. C. Murulana, M. Ozcan, F. Karadag, I. Dehri, I. B. Obot, E. E. Ebenso, *International Journal of Electrochemical Science* **7** (2012) 5035-5056.
[24] H. Elmsellem, H. Nacer, F. Halaimia, A. Aouniti, I. Lakehal, A. Chetouani, S. S. Al-Deyab, I. Warad, R. Touzani, B. Hammouti, *International Journal of Electrochemical Science* **9** (2014)5329-5351.
[25] G. H. Koch, M. P. H. Brongers, N. G. Thompson, Y. P. Virmani, J. H. Payer, Corrosion cost and preventive strategies, *NACE,* Houston TX, United States, (2002) 773.
[26] P. O. Ameh, P.U. Koha, N. O. Eddy, *Chemical Sciences Journal* **6** (2015) doi: 10.4172/2150-3494.1000100
[27] M. Y. Habibat, N. O. Eddy, J. F. Iyum, C. E. Gimba, E. E. Oguzie, *Chemical Material Research* **2** (2012) 1-12.
[28] R. Chami, M. Boudalia, S. Echihi, M. ElFal,A. Bellaouchou, A. Guenbour, M. Tabyaoui, E. M.Essassi, A. Zarrouk, Y. Ramli, *Journal of Materials and Environmental Sciences* **8** (2017) 4182-4192.
[29] G. Raja, K. Saravanan, S. Sivakumar, *Rasayan Journal of Chemistry* **8** (2015) 8-12.
[30] M. E. Mohammed, K. K. Taha, S. A. Khalil, S. A. Talab, *International Letters of Chemistry, Physics and Astronomy* **14** (2013) 87-102.
[31] M. Lebrini, M. Traisnel, M. Lagrenée, B. Mernari, F. Bentiss, *Corrosion Science* **50** (2008) 473-479.
[32] B. Tan, S. Zhang, W. Li, X. Zuo, Y. Qiang, L. Xu, J. Hao, S. Chen. *Journal of Industrial and Engineering Chemistry* **77** (2019) 449-460.
[33] A. A. Khadom, A. N. Abd, N. A. Ahmed*, South African Journal of Chemical Engineering* **25** (2018) 13-21.
[34] V. C. Anadebe, O. D. Onukwuli, M. Omotioma, N. A. Okafor, *South African Journal of Chemistry* **71** (2018) 51-61.
[35] T. He, W. Emori, R. H. Zhang, P. C. Okafor, M. Yang C. R. Cheng *Bioelectrochemistry,* **130** (2019) 107332-107342
[36] M. Ramezanzadeh, G. Bahlakeh, B. Ramezanzadeh, *Journal of Molecular Liquids* **292** (2019) 111387-111396.